Comparison of DMSP SSM/I and Landsat 7 ETM+ Sea Ice Concentrations During Summer Melt

D. J. Cavalieri[1], T. Markus[2], and A. Ivanoff[3]

[1]Laboratory for Hydrospheric Processes/Code 971
NASA Goddard Space Flight Center
Greenbelt, MD 20771
Telephone: +01-301-614-5901
Fax: +01-301-614-5644
Email: Donald.J.Cavalieri.1@gsfc.nasa.gov

[2]NASA Goddard Space Flight Center/UMBC JCET/Code 971
Greenbelt, MD 20771

[3]SSAI/NASA Goddard Space Flight Center/Code 971
Greenbelt, MD 20771

Submitted to the *Annals of Glaciology*

Significance

The significance of this paper is that it provides for the first time a quantitative measure of the errors incurred by the EOS Aqua AMSR-E sea ice concentration algorithm resulting from surface melt effects in the Arctic. Free water in the sea ice snow cover and melt ponds are currently the largest source of error in the determination of Arctic sea ice concentrations with satellite passive microwave sensors. Landsat 7 Enhanced Thematic Mapper (ETM+) images were used to provide an accurate estimate of actual sea ice concentrations. Results show that in areas of high melt ponding, the AMSR-E Arctic sea ice concentration retrievals underestimate sea ice concentrations by about 12% compared to the Landsat values, although agreement with the Landsat 7 sea ice concentration retrievals overall was good. Based on a linear regression analysis of 116 25-km samples, the correlation coefficient was 0.98 with an RMS error of 7.8%. This work supports NASA's EOS algorithm development and validation activities.

**Comparison of DMSP SSM/I and Landsat 7 ETM+
Sea Ice Concentrations During Summer Melt**

D. J. Cavalieri[1], T. Markus[2], and A. Ivanoff[3]

[1]Laboratory for Hydrospheric Processes/Code 971
NASA Goddard Space Flight Center
Greenbelt, MD 20771
Telephone: +01-301-614-5901
Fax: +01-301-614-5644
Email: Donald.J.Cavalieri.1@gsfc.nasa.gov

[2]NASA Goddard Space Flight Center/UMBC JCET/Code 971
Greenbelt, MD 20771

[3]SSAI/NASA Goddard Space Flight Center/Code 971
Greenbelt, MD 20771

Submitted to the *Annals of Glaciology*

Popular Summary

As part of NASA's EOS Aqua sea ice validation program for the Advanced Microwave Scanning Radiometer (AMSR-E), Landsat 7 Enhanced Thematic Mapper (ETM+) images were acquired to develop a sea ice concentration data set with which to validate the AMSR-E sea ice concentration algorithm. The standard AMSR-E Arctic sea ice concentration product will be obtained with the enhanced NASA Team (NT2) algorithm. The goal of this study is to assess the accuracy to which the NT2 algorithm, using DMSP Special Sensor Microwave Imager radiances, retrieves sea ice concentrations under summer melt conditions. Melt ponds are currently the largest source of error in the determination of Arctic sea ice concentrations with satellite passive microwave sensors. To accomplish this goal, Landsat 7 ETM+ images of Baffin Bay were acquired under clear sky conditions on the 26th and 27th of June 2000 and used to generate high-resolution sea ice concentration maps with which to compare the NT2 retrievals. Based on a linear regression analysis of 116 25-km samples, we find that overall the NT2 retrievals agree well with the Landsat concentrations. The regression analysis yields a correlation coefficient of 0.98. In areas of high melt ponding, the NT2 retrievals underestimate the sea ice concentrations by about 12% compared to the Landsat values.

Comparison of DMSP SSM/I and Landsat 7 ETM+ Sea Ice Concentrations During Summer Melt

D. J. Cavalieri[1], T. Markus[2], and A. Ivanoff[3]

[1]Laboratory for Hydrospheric Processes/Code 971

NASA Goddard Space Flight Center

Greenbelt, MD 20771

Telephone: +01-301-614-5901

Fax: +01-301-614-5644

Email: Donald.J.Cavalieri.1@gsfc.nasa.gov

[2]NASA Goddard Space Flight Center/UMBC JCET/Code 971

Greenbelt, MD 20771

[3]SSAI/NASA Goddard Space Flight Center/Code 971

Greenbelt, MD 20771

Submitted to the *Annals of Glaciology*, February 27, 2001

ABSTRACT. As part of NASA's EOS Aqua sea ice validation program for the Advanced Microwave Scanning Radiometer (AMSR-E), Landsat 7 Enhanced Thematic Mapper (ETM+) images were acquired to develop a sea ice concentration data set with which to validate AMSR-E sea ice concentration retrievals. The standard AMSR-E Arctic sea ice concentration product will be obtained with the enhanced NASA Team (NT2) algorithm. The goal of this study is to assess the accuracy to which the NT2 algorithm, using DMSP Special Sensor Microwave Imager radiances, retrieves sea ice concentrations under summer melt conditions. Melt ponds are currently the largest source of error in the determination of Arctic sea ice concentrations with satellite passive microwave sensors. To accomplish this goal, Landsat 7 ETM+ images of Baffin Bay were acquired under clear sky conditions on the 26th and 27th of June 2000 and used to generate high-resolution sea ice concentration maps with which to compare the NT2 retrievals. Based on a linear regression analysis of 116 25-km samples, we find that overall the NT2 retrievals agree well with the Landsat concentrations. The regression analysis yields a correlation coefficient of 0.98. In areas of high melt ponding, the NT2 retrievals underestimate the sea ice concentrations by about 12% compared to the Landsat values.

Introduction

High resolution, multispectral imagery obtained from the Landsat series of satellites continues to provide the best source of spaceborne data with which to validate sea ice concentration retrievals from satellite passive microwave radiometers. The limitations are, of course, the presence of clouds and polar darkness. Nonetheless, under favorable conditions Landsat imagery have been used successfully in numerous comparative studies with satellite passive microwave sea ice retrievals. It is the high-resolution capability of the Landsat visible and infrared sensors in particular that makes Landsat imagery a highly useful validation tool. One of the earliest studies was a comparison of Antarctic sea ice concentrations from Nimbus 5 ESMR with Landsat 1 and 2 Multispectral Scanner (MSS-7) near infrared imagery (Comiso and Zwally, 1982). In another study, Landsat MSS-7 imagery of the North Water area of Baffin Bay was used to validate Nimbus 7 Scanning Multichannel Microwave Radiometer sea ice concentrations (Steffen and Maslanik, 1988). As part of the Defense Meteorological Satellite Program Special Sensor Microwave/Imager (SSMI) sea ice validation effort, Landsat 5 MSS images were used for the validation of Arctic and Antarctic sea ice concentration retrievals during spring, summer, and fall (Steffen and Schweiger, 1991). Sea ice retrieval comparisons were

also made among NOAA AVHRR, Landsat MSS, and NASA aircraft microwave imagery (Emery and others, 1991). More recently, Landsat Thematic Mapper (TM) imagery have been used to identify sea ice types and surface features (Steffen and Heinrichs, 1994).

Landsat 7, the latest in the Landsat series of satellites was launched on April 15, 1999. It is in a circular, sun-synchronous orbit at an altitude of 705 km with an inclination of 98.2° and has a descending node equatorial crossing time of about 10 am. The Enhanced Thematic Mapper (ETM+) on Landsat 7 is an enhanced version of the TM flown on Landsat 4 and 5 and provides synoptic, high-resolution, multispectral imagery of the earth's surface with a swath width of 185 km. The instrument measures radiation in six spectral bands covering the visible to the shortwave infrared (Bands 1-5) at a spatial resolution of 30 m. There is also a 60-m resolution thermal infrared band (band 6) and a 15-m resolution panchromatic band (band 8). More detailed information on the Landsat 7 ETM+ and derived products are provided elsewhere (Parkinson and Greenstone, 2000).

Landsat 7 ETM+ imagery was acquired to develop a sea ice concentration data set with which to validate AMSR-E sea ice concentration algorithms. The standard AMSR-E Arctic sea ice

concentration product will be obtained with the enhanced NASA Team (NT2) algorithm (Markus and Cavalieri, 2000). In contrast to the original NASA Team (NT) algorithm (Cavalieri and others, 1984; Gloersen and Cavalieri, 1986), the NT2 algorithm provides weather-corrected sea ice concentrations through the use of both a wider range of microwave frequencies (18.7-89.0 GHz) and an atmospheric radiative transfer model. The goal of this study is to assess the accuracy to which the NT2 algorithm, using DMSP SSMI radiances, retrieves sea ice concentrations under summer melt conditions. Melt ponds are currently the largest source of error in the determination of Arctic sea ice concentrations with satellite passive microwave sensors. To accomplish this goal, Landsat 7 ETM+ images of Baffin Bay were acquired under clear sky conditions during late June 2000 and used to generate a high resolution sea ice concentration data set with which to compare the NT2 retrievals. ETM+ imagery provides high spatial resolution (15 m at band 8) and relatively wide spatial coverage (185 km).

Data and Analysis

Four Landsat 7 ETM+ scenes were obtained for the Baffin Bay region on June 26 and 27, 2000 (Figure 1). For each scene numbered 1 through 4, the scene ID, acquisition date, path, and row numbers are provided in Table 1. The panchromatic band

with a spectral range of 0.52 –0.90 μm was used to calculate sea ice concentrations, because it has twice the spatial resolution of the other bands (15 m vs 30 m). The variation in surface brightness in this spectral range with sea ice concentration, ice type, snow cover, and degree of surface melt has been studied from both observational as well as theoretical perspectives (e.g., Grenfell, 1983; Perovich and others, 1986; Grenfell and Perovich, 1986). It is this variation that permits sea ice parameters to be determined from the Landsat imagery. The four Landsat 7 ETM+ scenes used in this study are shown in Figure 2. Variations in observed surface brightness result from variations in sea ice concentration and from various stages of surface melt on the ice floes.

Methods employed to derive ice concentrations from Landsat imagery are determined by the ice conditions during a particular season. For example, in winter when ice types range from newly formed dark nilas to thick first-year ice with snow cover, the range of brightness over sea ice is largely a function of ice age, whereas during summer when no new ice is formed, the variations in brightness mainly result from variations in ice concentration and in the degree of ice surface melt. In this comparative study, the challenge is to discriminate between ice with surface melt and ice-free ocean. That is, we need to discriminate between melt ponds and ponds that have melted through the ice. At present we can not

make this discrimination with a high degree of accuracy. However, the number of 15-m Landsat pixels within a 25-km SSMI pixel is about 2.8 x 10^6 thus allowing for some error in this determination while still providing a useful degree of accuracy for the validation of the SSMI ice concentration retrievals at a 25-km resolution.

ETM+ sea ice concentrations were computed from the panchromatic band radiances on a 15-m resolution grid by applying a linear relationship between ice and water thresholds defined within the Digital Number (DN) value range 0-255. Histograms of DN values (0-255) for each of the four Landsat images shown in Figure 2 are provided in Figure 3. Each histogram exhibits a bimodal distribution. The lower (darker) mode corresponds to ice-free water and has a well-defined peak (centered at or near 15). The higher (brighter) mode spans a much broader range (100-200) and corresponds to sea ice with varying degrees of surface melt. For the purpose of calculating sea ice concentrations from the panchromatic imagery, we define two thresholds, one for ice-free ocean and one for ice-covered ocean.

Examination of open water areas shows that while most of these areas had grey-scale DN values centered near 15, higher open water values of up to 20 were also observed as a result of the

presence of very thin clouds. Thus, an open-water threshold of 20 was chosen to eliminate the possibility of thin clouds being classified as low ice concentration. The selection of the ice threshold was more difficult.

Based on an analysis of various subscenes of the Landsat imagery (Markus and others, this issue), the ice threshold was selected to be 60. Values below this threshold presumably represent either open water or a mixture of water and subresolution ice. Figure 4 shows a subscene of scene 2 (1711) where all pixels with DN values of 60 $\pm$ 4 are indicated in red. One can clearly see that the vast majority of these pixels are indeed sea ice pixels. Small areas of red are also observed between floes apparently indicating mixed-pixels (pixels with ice concentration less than 100%). Thus, we believe that an overestimate of ice concentration resulting from this choice of threshold is insignificant.

A linear interpolation between the water and ice thresholds provides a measure of ice concentration between identifiable ice floes. In summary, all 15-m ETM+ pixels with values greater than or equal to the ice threshold of 60 are classified as ice, pixels with values less than or equal to the ice-free ocean threshold of 20 are classified as water, and pixels with values between these two

thresholds have ice concentrations determined by a linear interpolation scheme.

The 15-m ice concentrations values were averaged over 25-km SSMI grids and then smoothed using a 3 by 3 25-km grid filter with each of the 9 filter cells having a specified weight to simulate the SSMI antenna pattern. Finally, those 25-km grids that were cloud covered were filtered from the data set by visually inspecting ETM+ band 5 (thermal infrared) imagery. The cloud filtered Landsat 7 ice concentrations were then compared with the SSMI ice concentrations derived with the NT2 sea ice algorithm.

Results

A total of 116 pairs of ice concentration values from the SSMI NT2 algorithm and from the Landsat ETM+ algorithm described in the previous section were compared. Based on a linear least squares regression analysis of these samples for Baffin Bay on June 26 and 27, 2000 (Figure 5), we find that the resulting linear correlation coefficient is 0.98. The RMS error is 7.8%.

The slope of the linear regression line in Figure 5 is consistent with the fact that passive microwave retrievals underestimate sea ice concentrations during summer melt. The cluster of points at the upper end of the scatter plot correspond to Landsat concentrations

greater than 90% with many greater than 95%. Most of the corresponding SSMI concentrations range from 80-90%. Many (27) of these high concentration values come from Landsat scene 1711 (Scene 2 in Figure 2). The average Landsat concentration for those 25-km cells within this scene is 97.2%, whereas the average SSMI concentration is 85.1%.

For the purpose of determining the sensitvity of these results on the particular selection of the ice threshold, we recomputed the Landsat concentrations using a more conservative ice threshold value of 70 instead of 60. In this case, the slope of the regression line was 0.914 and the intercept was 3.40. The correlation coefficient was 0.97. These differences are not significant. Furthermore, the computed Landsat ice area decreased from 59.7% to 56.8%, a change of less than 3%. The latter value is our estimate of the uncertainty in Landsat ice concentration retrievals and is consistent with earlier estimates of about 4% (Steffen and Schweiger, 1991).

Conclusions

Based on the analysis of four Landsat 7 ETM+ scenes of Baffin Bay on the 26 and 27 June 2000, we find that overall the SSMI sea ice concentration retrievals using the NT2 algorithm are quite good.

The overall correlation is 0.98. The NT2 algorithm underestimates ice concentrations in regions where there are high concentrations of melt ponding. This result is consistent with known limitations of passive microwave retrievals during summer melt conditions. In scene 2 (Table 1) where both the ETM+ ice concentration and melt pond density are high, the corresponding SSMI ice concentrations are lower by 12.1% on average. For all 116 ice concentration pairs, the RMS difference is 7.8%. At present there are no remedies for this underestimation with passive microwave sensors, but the combination of high resolution visible and infrared sensors together with the soon to be launched AMSR sensors on EOS Aqua and on ADEOS II with their higher spatial resolutions is expected to help.

Acknowledgements

We greatfully acknowledge the Landsat 7 Project for help with the acquisition of the ETM+ imagery and the National Snow and Ice Data Center for the SSMI polar stereographic brightness temperature grids. This work was supported by the NASA EOS Aqua Project.

References

Cavalieri, D. J., P. Gloersen, and W. J. Campbell. 1984. Determination of sea ice parameters with the Nimbus-7 SMMR, *J. Geophys. Res.*, **89**(D4), 5355 5369.

Comiso, J. C. and H. J. Zwally. 1982. Antarctic sea ice concentration inferred from Nimbus 5 ESMR and Landsat imagery, *J. Geophys. Res.*, **87**(C8), 5836 5844.

Emery, W. J., M. Radebaugh, C. W. Fowler, D. J. Cavalieri, K. Steffen. 1991. An intercomparison of sea ice parameters computed from AVHRR and Landsat satellite imagery and from airborne passive microwave radiometry, *J. Geophys. Res.*, **96**(C12), 21,971 21,987.

Gloersen P. and D. J. Cavalieri. 1986. Reduction of weather effects in the calculation of sea ice concentration from microwave radiances, *J. Geophys. Res.*, **91**(C3), 3913 3919.

Grenfell, T. C. 1983. A theoretical model of the optical properties of sea ice in the visible nad near infrared, *J. Geophys. Res.*, **88**(C14), 9723 9735.

Grenfell, T. C. and D. K. Perovich. 1986. Optical properties of ice and snow in the polar oceans. II: theoretical calculations, Proceedings of the Society of Photo-Optical Instrumentation Engineers, Ocean Optics VIII, **637**, 242 251.

Markus, T. and D. J. Cavalieri. 2000. An enhancement of the NASA Team sea ice algorithm, *IEEE Trans. Geosci. and Remote Sensing*, **38**(3), 1387 1398.

Markus, T., D. J. Cavalieri, and A. Ivanoff. 2001. The potential of using Landsat 7 data for the classification of sea ice surface conditions during summer, *Annals of Glaciology*, this issue.

Parkinson, C. L. and R. Greenstone. 2000. EOS Data Products Handbook, Vol. 2, NASA Goddard Space Flight Center, Greenbelt, MD 20771.

Perovich, D. K., G. A. Maykut, and T. C. Grenfell. 1986. Optical Propertiew of ice and show in the polar oceans. I: observations, Proceedings of the Society of Photo-Optical Instrumentation Engineers, Ocean Optics VIII, **637**, 232 241.

Steffen, K. and J. A. Maslanik. 1988. Comparison of Nimbus 7 scanning multichannel microwave radiometer radiance and derived

sea ice concentrations with Landsat imagery for the North Water area of Baffin Bay, *J. Geophys. Res.*, **93**(C9), 10,769 10,781.

Steffen, K. and A. Schweiger. 1991. NASA Team Algorithm for Sea Ice Concentration Retrieval From DMSP SSM/I: Comparison With Landsat Satellite Imagery, *J. Geophys. Res.*, **96**(C12), 21,971 21,987.

Steffen, K. and J. Heinrichs. 1994. Feasibility of sea ice typing with synthetic aperture radar (SAR): Merging of Landsat thematic mapper and ERS 1 SAR satellite imagery, *J. Geophys. Res.*, **99**(C11), 22,413 22,424.

Table 1. Landsat 7 ETM+ scenes of Baffin Bay for 26 and 27 June 2000 used in the comparison with SSMI NT2 sea ice concentration retrievals.

Scene No.	Scene ID	Acqusition Date	Path	Row
1	7017010000017850	June 26, 2000	17	10
2	7017011000017850	June 26, 2000	17	11
3	7024008000017951	June 27, 2000	24	08
4	7024009000017951	June 27, 2000	24	09

Figure Captions

Figure 1. Baffin Bay map showing the location of the four Landsat 7 ETM+ scenes.

Figure 2. The four Landsat 7 ETM+ scenes (Panchromatic Band 8) used in this study.

Figure 3. Histograms of DN values (0-255) for each of the four Landsat 7 ETM+ scenes.

Figure 4 Landsat 7 ETM+ (Band 8) subscene of scene 2 with DN values in the range 60 ± 4 indicated in red.

Figure 5. Scatter plot of sea ice concentrations derived from the DMSP SSMI and Landsat 7 ETM+ sensors.

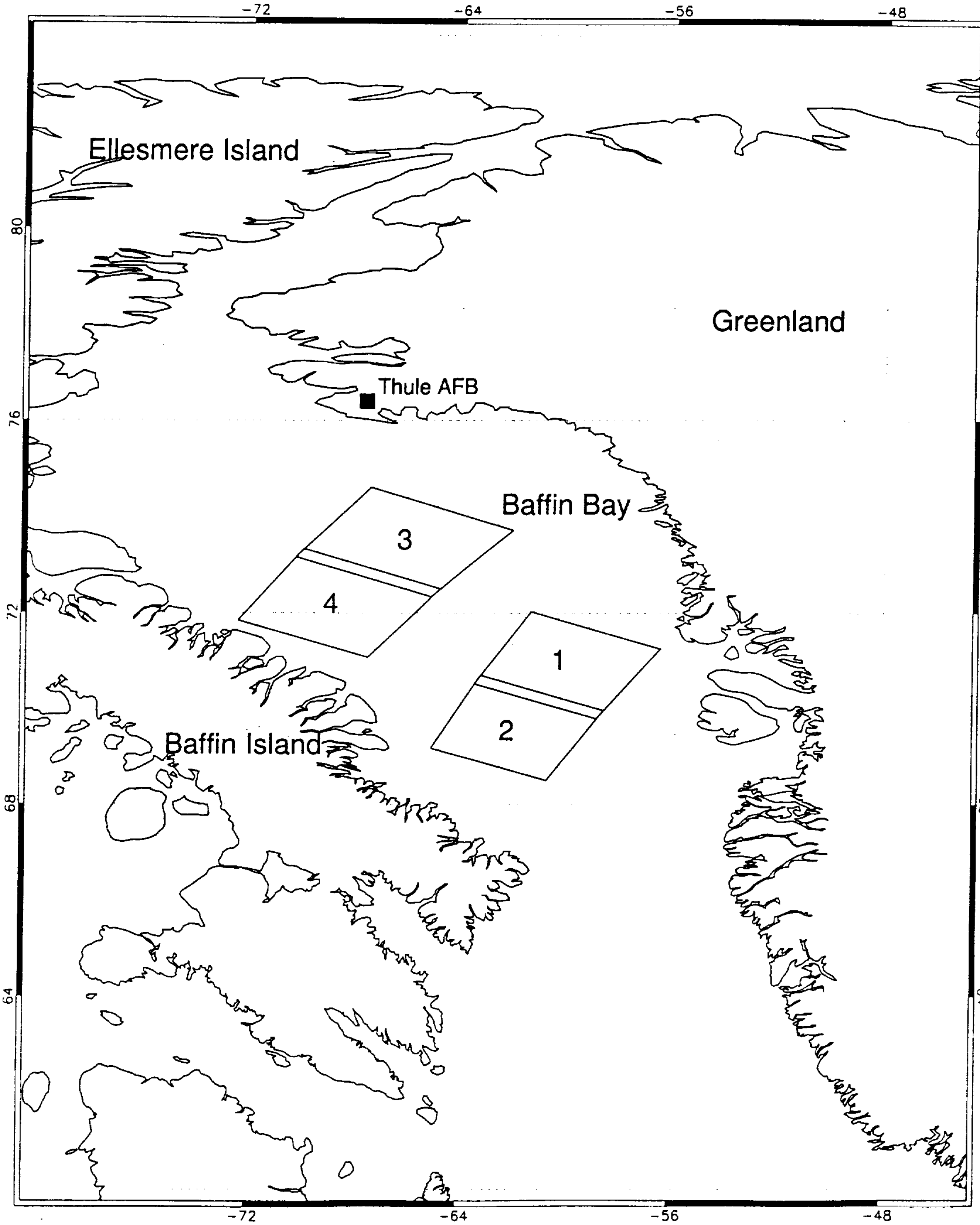
-72
-64
-56
-48
80
76
72
68
64
Ellesmere Island
Greenland
Thule AFB
Baffin Bay
3
4
1
2
Baffin Island

FIG 1

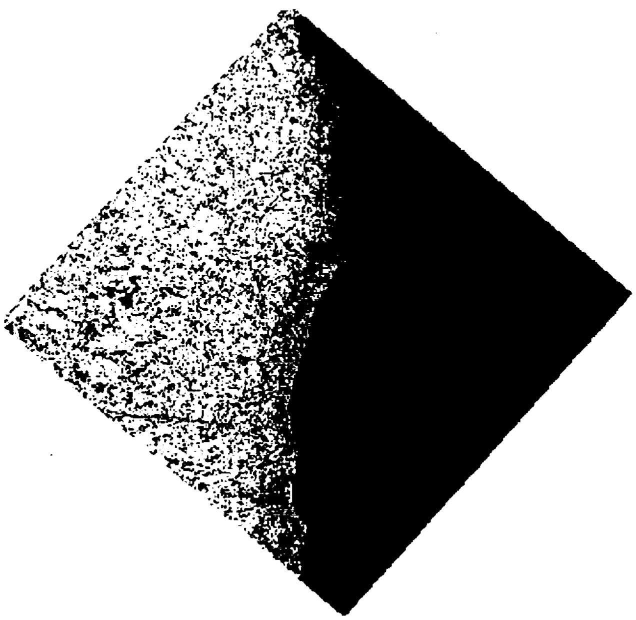

Scene 1

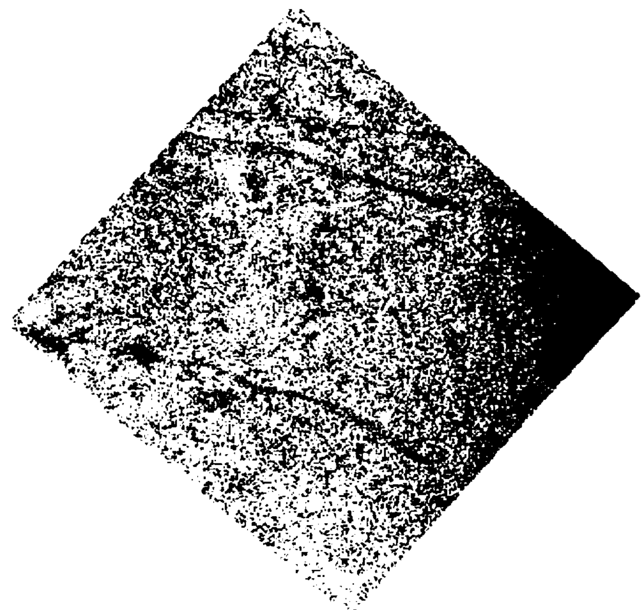

Scene 2

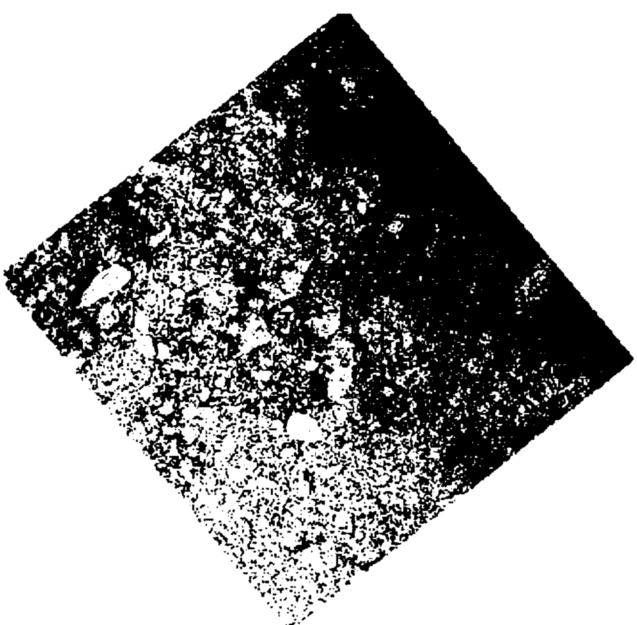

Scene 3

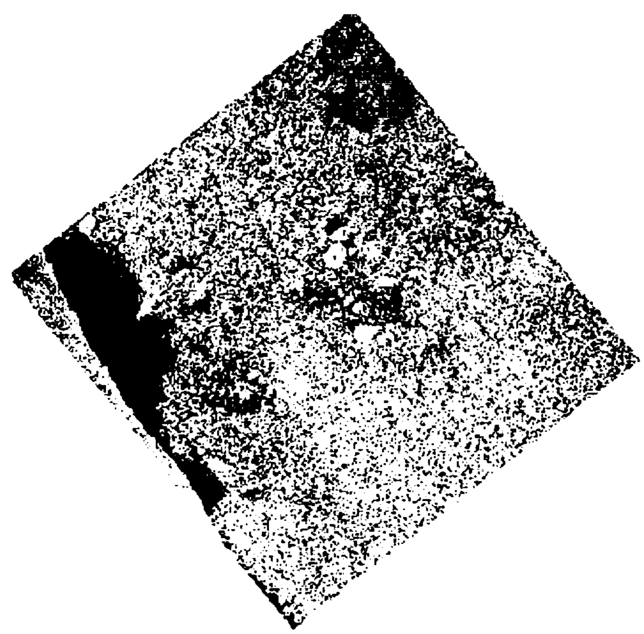

Scene 4

FIG. 2

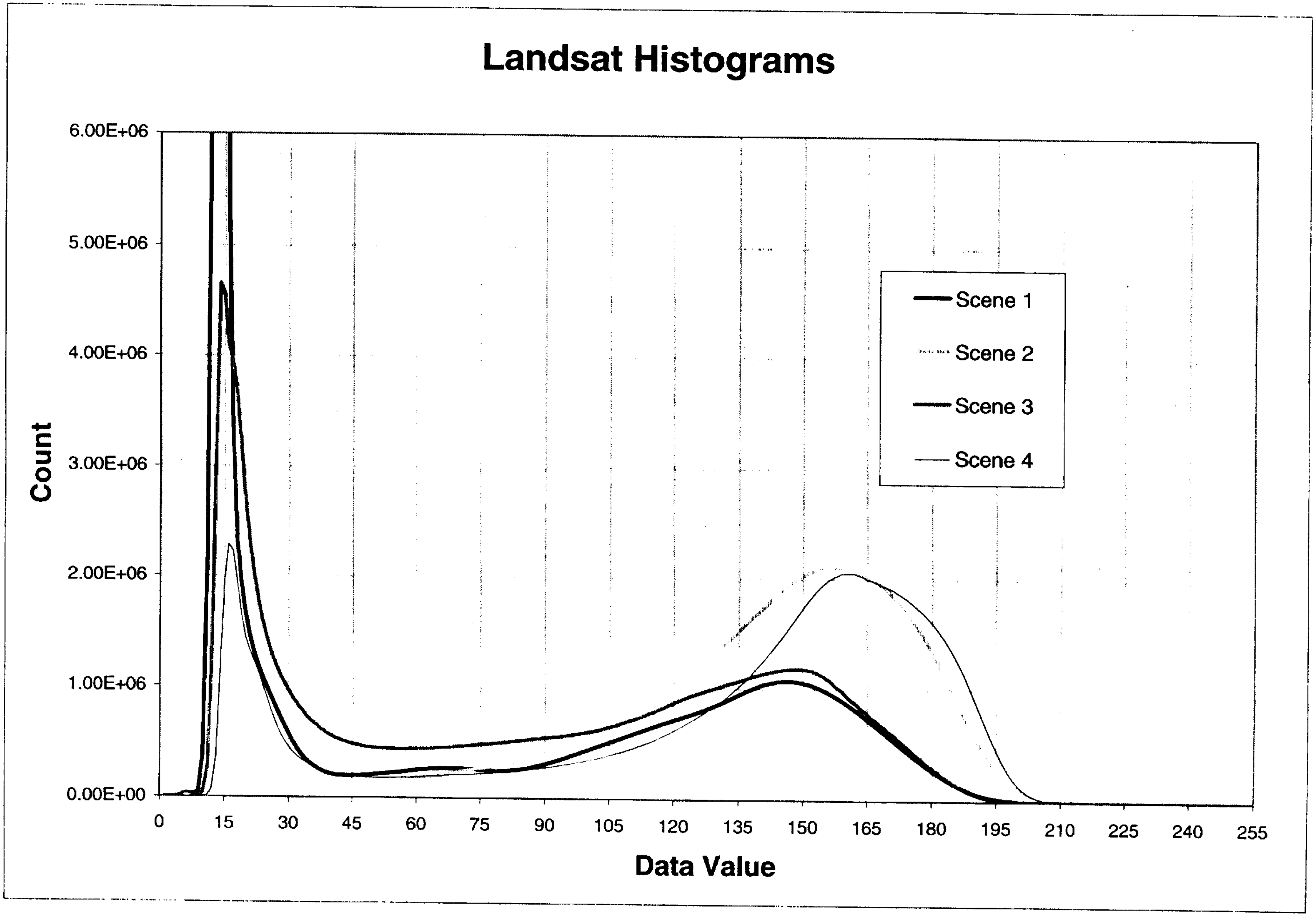
Landsat Histograms
Count
6.00E+06
5.00E+06
4.00E+06
3.00E+06
2.00E+06
1.00E+06
0.00E+00
0
15
30
45
60
75
90
105
120
135
150
165
180
195
210
225
240
255
Data Value
Scene 1
Scene 2
Scene 3
Scene 4

FIG 4

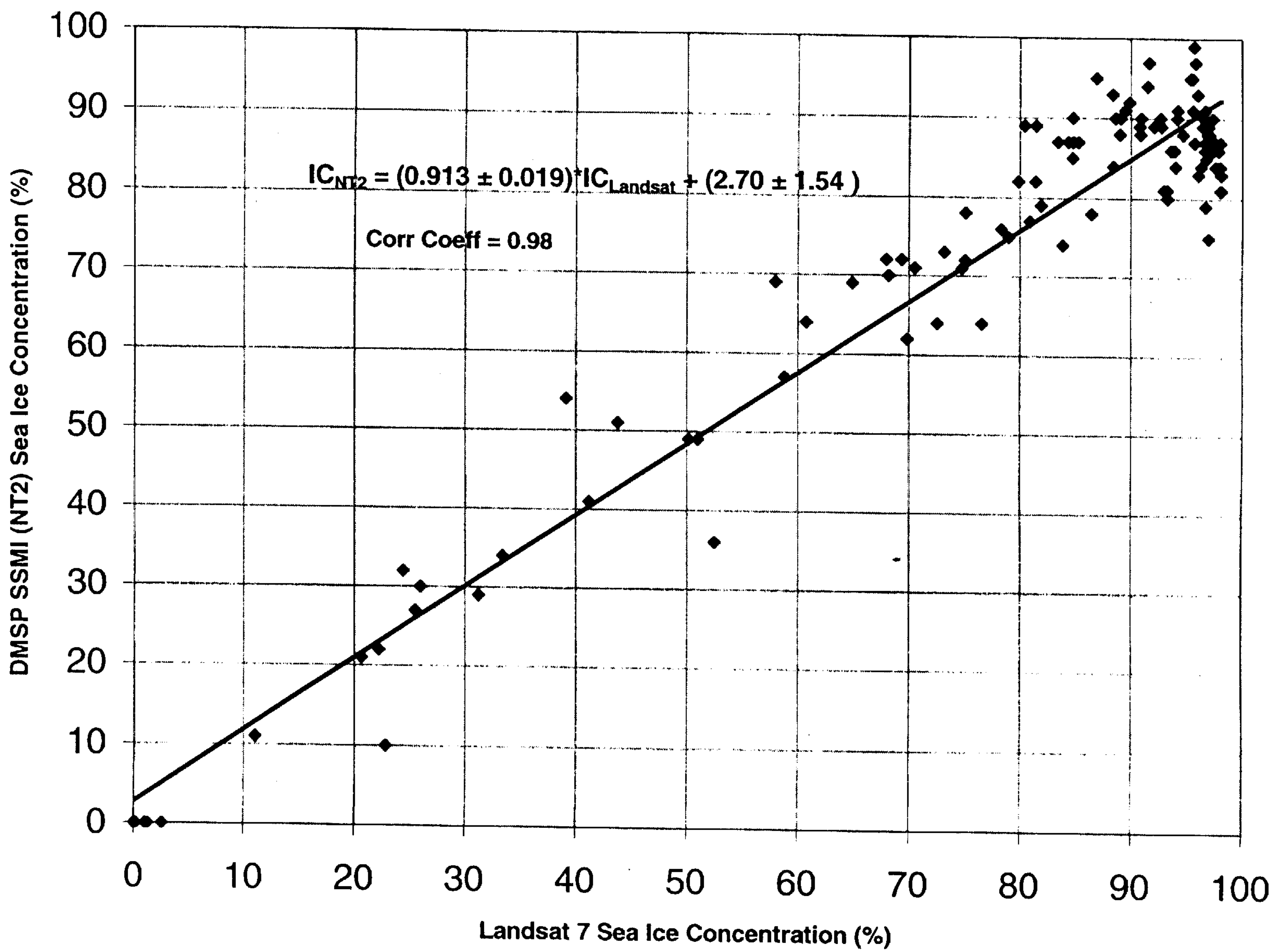

$IC_{NT2} = (0.913 \pm 0.019)*IC_{Landsat} + (2.70 \pm 1.54)$
Corr Coeff = 0.98
DMSP SSMI (NT2) Sea Ice Concentration (%)
Landsat 7 Sea Ice Concentration (%)
0
10
20
30
40
50
60
70
80
90
100

FIG. 5